ITT Industrial Laboratories, Ft. Wayne, Indiana

RESEARCH MEMO 401

DAYTIME STAR ACQUISITION AND TRACKING USING THE IMAGE DISSECTOR

E. H. Eberhardt
May 14, 1964

1.0 INTRODUCTION

This memo discusses the problem of locating and tracking a star within a certain optical field of view in daylight using an image dissector. The basic problem is to be able to identify the precise location of the star in the presence of an obscuring sky brightness background signal.

This memo is concerned only with the problem of daytime operation. At night or in space, the image dissector, because of its low dark noise, as pointed out by Salinger (Ref. 4) and Laverty (Ref. 5) becomes the method of choice.

2.0 DISSECTOR PERFORMANCE

In order to separate to the maximum degree possible the optical imaging problems, such as choice of optical aperture, lens speed, image size, etc. considered in Section 3.0 of this memo, from the tube detection problems proper, the input image geometry at the plane of dissector photocathode as shown in the following sketch will be assumed:

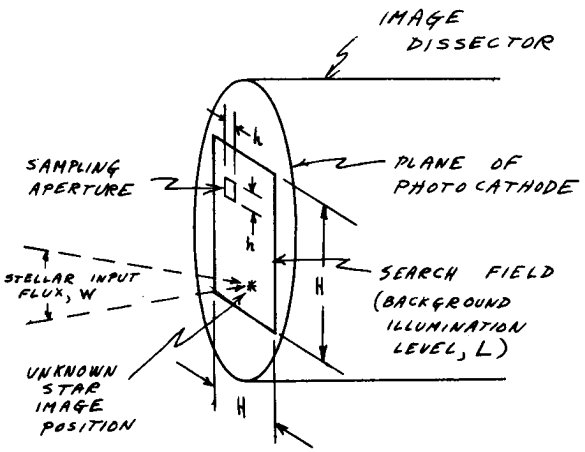

Figure 1 Image Field Parameters in Plane of Dissector Photocathode

It will also be assumed that an aperture or sampling element, h x h in size, is to be scanned electronically over the total search field area, H^2, in some programmed sequence, including all possible stellar flux locations. When the added flux, W, from the star to be located is detected in the output signal current from the dissector, the position of the aperture at that instant of time determines the unknown star position, terminating the search or acquisition mode. This search mode may then be followed by a tracking mode in which further position determination accuracy can be achieved and subsequent star motion followed through the field of view.

For simplification of this analysis, the usual continuous tv type raster line scan, will be assumed to be replaced by a jumped scan, in which each small image area, h x h, is observed for a small dwell time, t, and then the sampling aperture area, h x h, is jumped instantaneously to another (usually adjacent) area for the same time, t, etc. etc. This assumption of jumped scan is in fact quite rigorously applicable in theory, not only for image dissectors, but for other types of tv camera tubes (Ref. 1).

Because of the simplicity of image dissector action we can now write down the noise, signal, and signal-to-noise relationships as follows:

Where no star flux occurs, the aperture will collect a total number of electrons leading to an output count, n, during the dwell time, t, equal to

$$n = \epsilon L h^2 Q_{sk} t$$

where Q_{sk} is the quantum efficiency of the photocathode at the wavelength of the incident sky brightness photons involved (integrated over the spectral region involved), ϵ is the photoelectron counting efficiency of the dissector, and compatible units (See Section 4.2) are used for the various parameters.

If the number of counts, n, were exactly constant from one image element to the next there would, of course, be no difficulty in detecting a star, since, any increase in n, would mean an increased flux input, i.e. a star signal. Unfortunately this ideal situation never occurs, at least in the daytime, for there are always unavoidable sources of fluctuation in this background signal level during scan. In the limiting case, in which all fluctuations due to geometrical sky brightness variations, photocathode non-uniformities, photoelectron counting efficiency, etc. have been eliminated there will still be the fundamental statistical fluctuation of n (sometimes called background noise, shot noise, emission noise, etc.) which is proportional to the square root of n, i.e.:

$$\text{Statistical noise fluctuation} \cong \sqrt{n} = \sqrt{\epsilon L h^2 Q_{sk} t} \qquad (1)$$

For the image element which includes the stellar flux, W, the added electron count Δn for this element will be given by

$$\Delta n = \epsilon W Q_{st} t \qquad (2)$$

where it is assumed that all electrons from the star flux, W, enter the dissector aperture, and that Q_{st} is the quantum efficiency of the photocathode for the particular stellar flux spectral distribution involved.

The detection problem now resolves itself into detecting the change, Δn, in the counting rate due to the stellar flux over and above the random statistical fluctuations, $\sqrt{n}$. In other words a signal-to-noise ratio, S/N, can be expressed as:

$$S/N = (\Delta n)^2/n \qquad (3)$$

where the squared ratio is used in order to correspond more closely with the usual S/N power ratio. Substitution of the previously derived relationships Eq. 1 and Eq. 2 for Δn and $\sqrt{n}$ into Eq. 3 gives:

$$S/N = \frac{\epsilon W^2 Q_{st}^2 t}{L h^2 Q_{sk}} \qquad (4)$$

as the fundamental signal-to-noise ratio for a single interrogated image element.

If one assumes the most efficient search possible, i.e. where each element is interrogated or examined once and once only (no overlap of areas), then the available dwell time, t, is given by

$$t = \left(\frac{h}{H}\right)^2 T$$

where T is the total search time, divided equally among all searched elemental areas.

The S/N ratio then reduces to

$$\frac{S}{N} = \frac{\epsilon W^2 Q_{st}^2 T}{L H^2 Q_{sk}} \qquad (5)$$

This is the final relation for the S/N ratio in terms of dissector and image plane parameters. If one substitutes known values of the seven parameters appearing, the ability of the dissector to detect a specified star can be predicted from this equation. This prediction can be expected to be reasonably reliable (See Section 2.3).

Four of these parameters, the stellar flux, W, the permissible search time, T, the sky brightness background illumination, L, and searched area, H^2, are essentially predetermined by the conditions on the problem, i. e. the type of star, time of day, optics selected, etc. to be discussed in Section 3.0 of this memo. The principal dissector design parameters available for choice are the cathode quantum efficiencies, Q_{st} and Q_{sk} and counting efficiency, ϵ.

2.1 Choice of Dissector Aperture Size

It is quite surprising to note from Eq. 5 that, under the assumed conditions, the ability of an image dissector to locate the unknown star position is independent of the dissector aperture dimensions, h x h. The choice of aperture size must therefore depend on other system requirements, such as the desired star position accuracy. Surprisingly enough this positional accuracy can be as high as desired without a sacrifice in S/N ratio, within the assumptions of the problem.

One assumption is that the aperture must be large enough to collect all or nearly all of the photoelectrons from the stellar flux signal, W. In electrostatically focused star tracker tubes (actually low resolution image dissectors) such as the ITTIL FW-118, FW-129, FW-130, F4003, F4004, etc. the smallest practical paraxial size for the dimension, h, without loss appears at present to be about 0.005 inch, and this dimension increases rapidly off-axis (See ITTIL Applications Note E3). For magnetically focused dissectors such as the ITTIL FW-125, FW-146, F4010, F4011, and F4012, the minimum aperture size can be reduced to about 0.0005 inch to 0.001 inch on axis depending somewhat on permissible scan power, an improvement of about 50 to 100 times in positional determination accuracy without special tracking modes over the star tracker tubes. This reduced size can be maintained over comparatively large image areas. In terms of the resulting image fields of view for these various dissector tubes, these apertures represent star area locations within one part in 10^3 to 1 part in 10^7.

Another limitation is introduced by the necessity for some overlap between sampled target elements, for example between scan lines, in order to avoid loss of star signal at the boundaries between nominally adjacent elements. For very small apertures this overlap may lead to excessive percentage overlap, with resultant reduced S/N ratio.

Small apertures also require faster scan rates, wider bandwidths for the associated circuits, more scan power, greater circuit stability, etc. Other practical considerations in the choice of aperture size will include such parameters as sky brightness gradients, photocathode microstructure, etc. In general it appears that a combination of these secondary considerations will control the choice of aperture size rather than the S/N ratio.

2.2 Choice of Aperture Shape

The image dissector is quite unique in its adaptability to various aperture shapes. If desired, a rectangular aperture can be used, or even an aperture

with cross hairs or special reticles to introduce various signal selecting scan patterns. One example would be a "wagon wheel" type aperture, nutated electrically during scan to convert the usual star signal to a possibly-easier-to-process FM signal. It appears that these special techniques may allow closer approach to the limiting S/N ratio computed above than other less sophisticated methods.

2.3 Achievement of Limiting Sensitivity

The dissector performance computed herein is based on the assumption that the dissector can "see" and be limited by the statistical fluctuation of the background photoelectron emission count. Actually, this statistical count fluctuation is equivalent mathematically (Ref. 2) to the more commonly encountered shot noise law (Ref. 3):

$$i_n^2 = 2 e \mu k I_{dc} \Delta f \qquad (6)$$

where i_n is the anode noise current associated with an average anode current, I_{dc}, a bandwidth, Δf, the electronic charge, e, a multiplier gain, μ, and a multiplier noise factor, k. Multiplier phototubes, and the image dissector multiplier phototube in particular, are, in fact, capable of direct observation of this basic shot noise current, modified by the multiplier noise factor, k, (Ref. 3).

For "perfect" multipliers, the noise factor, k, is given by

$$k = \frac{\sigma}{\sigma - 1} \qquad (7)$$

where σ = the average gain/stage of the multiplier, giving, for $\sigma = 5$, $k = 1.25$, or a 25 percent increase in the noise. Thus "perfect" image dissectors should approach within about 80 percent of the S/N performance computed herein. In practice, we have shown that this close approach to limiting shot noise can be expected in properly designed tubes. The dissector, in fact, is quite unique among scanning detectors in this ability to "see" and be limited by the fundamental photoemission shot noise. While this fundamental noise may be excessive in dissectors for tv studio type applications, it does allow accurate analysis of expected dissector performance, as in this memo.

It should not be assumed, however, that all dissectors, regardless of design will approach the limiting performance. Dissectors with low gain multipliers, low current output capabilities, low photocathode average emission current density limits, or noisy electron multipliers may not achieve the S/N ratio computed herein. In particular, channel multiplier techniques, as opposed to discrete stage multipliers, do not presently appear to be capable of achieving the desired performance characteristics.

Surprisingly enough, there are sound technical reasons to believe that there are possibilities for new "smoothing multiplier" image dissectors in which the effective noise bandwidth, Δf, in Eq. 6 can be reduced, thus reducing the disturbing shot noise current, i_n, without loss of position determination accuracy, i.e. resolution. These new techniques, which hold considerable promise for advanced low noise image dissectors, are described in Ref. 11.

2.4 Dark Noise and Other Limitations

There may be other sources of disturbing "noise" in dissector systems, such as:

1. Photocathode inhomogeneities
2. Dark noise, either tube or circuit
3. Noise-in-signal (fluctuation of the actual flux to be detected)
4. Gain drift, etc.

H. Salinger, (Ref. 4) has shown that (2) and (3) are nearly always negligible for the daytime search or acquisition mode considered here. This follows from the high level of image background illumination normally encountered for daytime search. At night, or under tracking conditions as opposed to search, tube dark noise or noise-in-signal may be significant parameters. Gain drift, (4) can be expected to be negligible for the short acquisition times involved though it may present calibration problems. This leaves cathode inhomogeneities as a possible major source of false star acquisition. Experimental studies at ITTIL indicate clearly that these inhomogeneities can be markedly reduced and possibly made negligible by a simple improvement of cleanliness and cathode processing control procedures. Furthermore, most of these inhomogeneities have sizes, polarities, and shapes which are clearly not attributable to a star flux input. For maximum acquisition accuracy it will undoubtedly be necessary to choose discrimination circuits which reject inhomogeneities of improper size, shape, polarity, etc.

2.5 Multiple Aperture Dissectors

The above computation assumes one aperture and one electron multiplier. Multiple aperture dissectors with or without corresponding separate multipliers are feasible and have been constructed and tested at ITTIL. Such dissectors open up entirely new possibilities for star search, though the basic S/N computations from this memo can be modified for application to these more complex dissectors.

One particularly attractive possibility would be to use a dissector with two close-spaced apertures and

two separate electron multipliers, observing only the difference signal in the two output leads. This technique would effectively suppress gradual variations in sky brightness or photocathode sensitivity (i.e. shading).

It should be noted that this differential comparison technique is also possible with a conventional single aperture dissector, possibly at some cost of S/N ratio, by the use of a wobbled scan, i.e. a scan which has a small vertical scan motion superimposed onto the primary horizontal line scan. A differential star signal would then appear as an amplitude fluctuation at the wobbling frequency (moving off and on the star flux area during one cycle of the wobble frequency).

2.6 Complex Scan Techniques

Unlike ordinary tv camera tubes such as the image orthicon and vidicon in which a repetitive constant scan pattern is required to establish the proper charge storage, write, and read cycling operation, image dissector scan can be modified from time to time in any way desired without interference with the available signal output level. As a matter of fact the dissector scan can be stopped entirely and the tube operated in the dc readout mode as a high gain ultrasensitive multiplier phototube.

This versatility of scan choice allows considerable freedom in the selection of optimum scanning techniques. For example, one fast pre-scan raster might be used to locate the most probable star locations, followed by a slower detailed examination of these individual expected locations only, for positive identification of the element actually including the star flux input.

A related advantage of the dissector is that it is not sensitive to star image motion, which tends to smear the stored information in such devices, as the vidicon and image orthicon, and reduce both sensitivity and accuracy of image location. The image dissector can therefore be used with a single slow search scan, compared to the more rapid multiple scans needed for the vidicon-orthicon devices.

2.7 Noise Bandwidth and Related Parameters

The usual concepts of noise bandwidth, Δf, noise current, i_n, and dc current, I_{dc}, in the shot noise relationship, Eq. 6, have been bypassed, so-to-speak, in this analysis. These concepts are, of course, directly related to and can be derived from the statistical fluctuation, Δn, of the counting rate, n, if so desired, leading to the same results found herein (Ref. 2). There are certain "hidden" assumptions however, contained in this present anslysis which might be pointed out. For example, the bandwidth of the monitoring circuits must be wide enough to be able to distinguish between the signal counting rate, n_2, in one sampled element, from the signal counting rates, n_1 and n_3 in the preceding and following elements without "cross-talk" and without amplifier noise becoming significant. With fast scan rates (i.e. small apertures and short search times) this may involve circuit design problems.

2.8 Cathode Fatigue

Operation of any photoemissive surface exposed to daylight can lead to excessive emitted photocurrent with subsequent fatigue (loss of cathode sensitivity). In general the average emission current limit is about 1-10 $\mu a/cm^2$ if tube life is to be many hours. For the large "f" number lens usually used for star search (see numerical examples) and the short operating life (usually a few seconds), cathode fatigue should not be serious. For long time star tracking cathode illumination limits must be observed.

2.9 Maximum Anode Current

With the high gain multipliers required in order to count individual photoelectrons large dissector apertures at high light levels can lead to anode output current saturation. This space charge saturation limitation does restrict the choice of search aperture to the smaller values, but these are normally desired in any case for star location accuracy.

2.10 Counting Efficiency

The concept of counting efficiency as utilized herein is somewhat new to image dissector performance analyses, although it has been applied by several experimenters to ultra low noise multiplier phototube performance (see references cited in Ref. 6). In brief, the counting efficiency, ϵ, is just the ratio of the number of countable output pulses in the dissector anode circuit to the number of triggering photoelectrons. The output pulses may be individually counted, or they may be allowed to merge into the more usual fluctuating output current and appear as anode shot noise. For properly designed dissectors, absolute counting efficiency ratios as high as 0.8 to 0.9 can reasonably be expected. For the less well designed devices, noted in Section 2.3, this ratio may be quite low and represents a serious loss of sensitivity.

3.0 OPTICAL SYSTEM PERFORMANCE

In Section 2.0 of this memo, the characteristics of an image dissector for star acquisition were discussed, assuming certain image field characteristics in the plane of the photocathode. These image field characteristics are related to the viewed stellar field and the selected optical system as shown in Figure 2.

The image field illumination, L, is related to the sky "brightness", B, by the relationship:

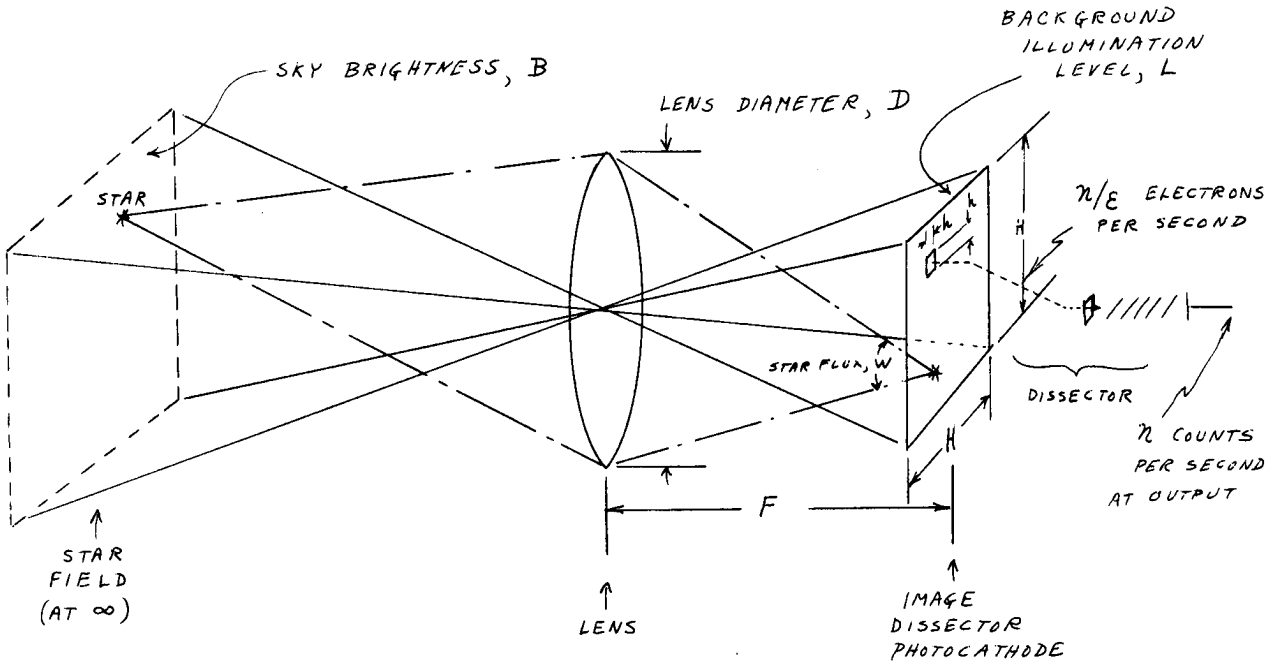

Figure 2 Optical Field Parameters

$$\frac{L}{B} = \frac{1}{4f^2} \quad * \qquad (8)$$

where f is the effective "f"/number of the lens. This "f"/number is, in turn, related to the effective lens diameter, D, and focal length, F, by the identity:

$$f = F/D \qquad (9)$$

In addition, the focal length F, is related to the field of view angle **, θ, and image field dimension, H, by:

$$\tan \theta/2 = \frac{H}{2F} \qquad (10)$$

or $$F \cong H/\theta \qquad (10a)$$

---

* This equation is numerically correct only if appropriate and corresponding paired units are used for "brightness", B, and illumination, L. Suitable pairs of units would be foot lamberts and foot candles, lamberts and phots, apostilbs and lux, etc., depending on the area units involved (ft^2, cm^2, and m^2 respectively). If true brightness units, such as candles/unit area or lumens/unit area/steradian, are used to express B, then the appropriate numerical factor of π must be included in Eq. 8.

** For simplicity the view field was assumed to be square in Figure 1. Other geometrics can of course be readily substituted.

Another simple relationship needed is that between the stellar image flux, W, and the stellar illumination level, I, at the plane of the optics, namely:

$$W = \frac{\pi D^2}{4} I \qquad (11)$$

Substitution of the above relationships into the S/N equation 5, gives for the fundamental S/N equation in terms of image dissector and stellar field parameters:

$$S/N = \frac{\epsilon (\pi DIQ_{st})^2 T}{4\theta^2 BQ_{sk}} \qquad (12)$$

A number of useful conclusions regarding the stellar acquisition problem can be derived from examination of this equation:

3.1 Choice of Optics

As far as the choice of optics is concerned the only directly appearing parameter in Eq. 12 is the effective lens diameter, D, which must clearly be as large as possible for maximum sensitivity. A secondary and hidden restriction in Eq. 12 is that the focal length of the lens must be chosen to yield the proper image field dimension, H, on the detector, for a given view angle, θ. As shown by the numerical examples listed later on in this memo, this restriction normally leads to a large focal length and rather surprisingly to a relatively "slow" lens speed, but larger or smaller detector fields can be selected without loss of sensitivity. Although lens "speed" does determine the background field illumination, L, the area, H^2, to be

searched by the image dissector also varies in such a way with fixed aperture diameter, D, as to just cancel out the change in noise with field illumination level due to a change in lens speed. Lens speed, per se, is therefore not a significant parameter or an image dissector star tracker.

Further restrictions on the choice of optics follow from the necessity that all of the star flux, W, must be focused to an area smaller than the selected dissector aperture size (but, of course, this aperture size choice itself is comparatively unrestricted, see Section 2.0), and the lens must yield the desired image quality as regards distortion, vignetting, aberrations, etc.

4.0 GENERAL OBSERVATIONS

4.1 Spectral Response, Filtering, and Cathode Quantum Efficiency Consideration

From Eq. 12 it follows that the effective star search sensitivity is proportional to the ratio

$$\frac{I^2 Q_{st}^2}{BQ_{sk}}$$

where the sensitivity products IQ_{st} and BQ_{sk} for stellar and sky flux respectively, contain all spectral response modifications due to selective atmospheric absorption, choice of photocathode, view angle with respect to the sun, etc. It has been suggested many times that selective optical filtering be used to improve the system performance by making use of the possibly small but unavoidable differences in spectral distribution which occur between stellar and sky brightness flux. However, since the product IQ_{st} enters as a squared parameter, while BQ_{sk} is linear only, it follows that it will usually be preferable in practice to maximize the sensitivity product, IQ_{st}, for the stellar flux, even though an apparent excess sensitivity, BQ_{sk}, to sky brightness flux may thereby result. This conclusion confirms the statement by Laverty (Ref. 5) that spectral filtering is seldom worthwhile in practice.

4.2 Choice of Units

Eq. 12 was derived on the basis of a certain numerical signal count per dwell time, t, compared to a certain statistical fluctuation count in the background count for the same dwell time. Eq. 12 must therefore be a dimensionless ratio based on numerical counting rates at the dissector output. The units of all parameters used in computing an S/N ratio from Eq. 12 must therefore be compatible with this counting concept. For example, if lumens,* centimeters, coulombs, and seconds are selected as the fundamental units, then the derived units listed in Appendix I must be used for the various parameters. The only unusual unit appearing in this system is the cathode quantum efficiency in electrons/lumen-second, in contrast with the more usual electrons/photon unit. However, cathode luminous sensitivity data in microamperes/lumen can be converted readily to the required values by dividing by 1.6×10^{-13}. Unfortunately μa/lumen cathode sensitivity figures are readily available only for input flux having a spectral distribution equivalent to a 2870° K color temperature tungsten lamp, which is hardly applicable to this stellar detection problem. Table I shows the computed ratio of luminous cathode sensitivity to the various spectral sources listed, compared to the standard 2870° K sensitivity for several JEDEC registered types of photocathodes.

* All commonly used photometric units can be expressed in terms of lumens plus the appropriate length, area and time dimensions.

TABLE I

Computed ratio of cathode luminous sensitivity (for the spectral distribution listed) to cathode luminous sensitivity (for 2870° K color temperature radiation).

Source	Type Photocathode S1*	S11*	S20*
5000° K black body	0.50	1.84	1.27
Mean solar flux	0.39	1.74	1.18
Daytime sky (Ref. 10)	---	---	1.91
P4* phosphor	0.11	1.94	1.12
P11* phosphor	0.16	5.4	2.74
P20* phosphor	0.083	0.69	0.51
NaI Scintillator (Harshaw data)	1.72	22.8	12.3

* Registered JEDEC spectral response distribution.

It can be seen that the luminous sensitivity of S-20 photocathodes is higher for "blue" sources, as usually encountered in stellar search problems.

4.3 Star Acquisition Versus Star Tracking

Upon first examination it might appear that star tracking (i.e. following a star as it moves through the field of view) is quite different from the star acquisition problem under consideration here, since, in star tracking, one can adopt a simpler scan pattern, such as the ITTIL rosette type scan (Ref. 7), in which one examines only a few "picture" elements surrounding the previously determined star location to see whether or not it has moved since the last scan.

However, since the S/N ratio in either mode is independent of the instantaneously examined element size, as noted in Section 2.1, there is inherently no difference in the two modes as far as application of the results of this analysis is concerned, though there may, of course, be numerical differences in the computed S/N ratio. In tracking modes in general, one will be dealing with only a few "picture" elements, a comparatively small* view field angle, θ and possibly a rather short repetition time, T, compared to acquisition modes, but, assuming that the appropriate numerical value of θ and T are substituted into the S/N Eq. 5 or 12, the ability to track as well as search, can be predicted. Both acquisition and tracking sensitivity is clearly proportional to T/θ^2:

$$\text{S/N (track or search)} \sim T/\theta^2$$

It seems likely that the effective S/N ratio during track may be somewhat higher than indicated by the S/N equations computed herein, since there will be many repetitive scan frames involved, permitting frame-by-frame comparisons to help differentiate star signal from random noise.

5.0 NUMERICAL EXAMPLES

It is instructive to insert into the S/N Eqs., 5 and 12, some typical numerical data. To do this it is convenient to make use of the approximate relationship given by Allen (Ref. 8) between stellar magnitude, m, and star illumination, I, in lumens/cm^2 (i.e. phots):

$$I = 0.8 \times 2.65 \times 10^{-10} \times 10^{-0.4m} \qquad (13)$$

where a factor of 0.8 is included to correct for atmospheric absorption.

A further assumption will be that we are using an S-20 photocathode with a 150 μa/lumen sensitivity, so that the two effective cathode efficiencies Q_{st} and Q_{sk}, assuming we are tracking a star of the same spectral class as the sun, will be (using Table I):

$$Q_{st} = \frac{(1.18)(150)}{1.6 \times 10^{-19} \times 10^{6}}$$

$$= 1.1 \times 10^{15} \text{ electrons/lumen second}$$

$$Q_{sk} = \frac{(1.91)(150)}{1.6 \times 10^{-19} \times 10^{6}}$$

$$= 1.79 \times 10^{15} \text{ electrons/lumen second}$$

A final numerical assumption will be that an absolute counting efficiency ratio, ϵ, of 0.9 has been achieved (See Paragraph 2.10).

* During track, the star can be followed in general through a larger field of view, as limited by the dissector photocathode, gimbal movement, vehicle window etc.

With these assumptions the following specific cases are of interest:

5.1 General Star Search Problem (Laverty data, Ref. 5, page 195)

D = 2.5 inches = 6.35 cm

θ = 1/2° = 8.73×10^{-3} radians

W = 4.13×10^{-10} lumens

B = 300 ft. lamberts = 0.322 lamberts

These data give:

$$I = \frac{4.13 \times 10^{-10} \times 4}{\pi (6.35)^2}$$

$$= 1.26 \times 10^{-11} \text{ phots.}$$

Assuming an arbitrary search time of 1 second, Eq. 12 gives:

$$S/N = \frac{0.9 \times (3.14 \times 6.35 \times 1.26 \times 10^{-11} \times 1.1 \times 10^{15})^2 \times 1.0}{4 \times (8.73 \times 10^{-3})^2 \times 0.322 \times 1.79 \times 10^{15}}$$

$$\cong 0.4$$

This is not a useful S/N ratio; in other words, dissectors cannot be expected to acquire a star under the stated operating conditions. Relatively small changes in the operating conditions, such as an increase in the search time to 10 seconds, will, however, offer image dissector possibilities.

It might be noted that Laverty's comment, in Ref. 5, that "the ratio of the luminous energy from the sky background is five orders of magnitude higher than that from the star" in this example, while technically correct, is not a propos since the star flux is directed geometrically to a point image, while the sky brightness flux is distributed over the full search field area.

5.2 Vidicon Tracker, Laverty Data (Ref. 5 page 204)

D = 1.6 inches = 4.1 cm

θ = 15 ft = 4.4×10^{-3} radians

T = 0.25 sec (assuming one frame acquisition)

m = 2.19 (Polaris)

B = 400 ft. Lamberts = 0.43 lamberts

from which I = 2.85×10^{-11} phots and

$$S/N = \frac{0.9 \times (3.14 \times 4.1 \times 2.85 \times 10^{-11} \times 1.1 \times 10^{15})^2 \times (0.25)}{4 \times (4.4 \times 10^{-3})^2 \times 0.43 \times 1.79 \times 10^{15}}$$

$$\cong 0.62.$$

This numerical value is to be compared with the experimentally determined value of $(9)^2 = 81$ for the vidicon tracker listed by Laverty. It can be seen that the image dissector would not perform properly under these specific operating conditions. If the search time can be increased to 2.5 seconds the resulting S/N ratio of 6.2 would, however, offer significant possibilities.

5.3 Image Orthicon, Laverty Data (Ref. 5 page 204 - 205)

$B = 1200$ ft lamberts $= 1.29$ lamberts

$\theta = 13$ ft $= 3.8 \times 10^{-3}$ radians

$D = 2.37$ inches $= 6.02$ cm

$F = 64$ inches $= 162$ cm

$m = -3.1$

$T = 0.25$ (one frame acquisition)

giving $I = 3.64 \times 10^{-9}$ phots and

$$S/N = \frac{0.9 \times (3.14 \times 6.02 \times 3.64 \times 10^{-9} \times 1.1 \times 10^{15})^2 \times 0.25}{4 \times (3.8 \times 10^{-3})^2 \times 1.29 \times 1.79 \times 10^{15}}$$

$$= 10,000$$

For a star as bright as this (-3.1 magnitude) it can be seen that the dissector should far exceed the capability of the image orthicon whose measured S/N ratio was $(6)^2 = 36$.

Recent successes in tracking the planet Venus under conditions almost identical with this example (Ref. 9) using an ITTIL dissector type star tracker (the FW-118) also confirm this conclusion.

5.4 Mechanical Tracker, Laverty Data (Ref. 5 page 203 - 204)

$D = 2$ inches $= 5.1$ cm

θ (track) $= 2$ ft $= 5.8 \times 10^{-4}$ radians

T (track) $= 2$ sec

m (gamma Gemini) $= 1.93$

$B = 1200$ ft. lamberts $= 1.29$ lamberts

giving $I = 3.6 \times 10^{-11}$ phots and

$$S/N = \frac{0.9 \times (3.14 \times 5.1 \times 3.6 \times 10^{-11} \times 1.1 \times 10^{15})^2 \, (2)}{4 \times (5.8 \times 10^{-4})^2 \times 1.29 \times 1.79 \times 10^{15}}$$

$$= 230$$

This computed S/N ratio compares favorably, as it should, since the dissector is merely a multiplier phototube with electronic scan, with the value of $(23.8)^2 = 570$ measured by Laverty for the mechanical scanner. An image dissector should in fact accomplish the same purposes as the mechanical scanner, but with greater system versatility and speed.

For the mechanical search mode reported by Laverty the time, T, was 10 minutes or 600 seconds and the search field angle θ was $1/2^o$ or 30 minutes of arc, giving

$$T/\theta^2 = 600/900 = 0.67$$

compared to

$$T/\theta^2 = 2/4 = 0.5$$

for the above track mode. Thus, a dissector should also perform both of these operations at approximately the same S/N ratio.

6.0 CONCLUSIONS

The image dissector appears to be capable of performance somewhat closer to that of competitive storage devices than may be apparent based on the ideal capabilities of these storage devices. While the dissector compares favorably with mechanical scanners, and exceeds the capabilities of the experimental image orthicon tracker cited, it does not compare favorably with the vidicon experimental tracker, at least for single frame acquisition. Whether or not slower frame times, multiple apertures dissectors, smoothing multiplier dissectors, image analysis techniques, FM modulation, or other specialized techniques can be used to improve dissector performance remains to be investigated.

REFERENCES

1. ITTIL Research Memo 246: "Photoconductive Camera Tube Theory".

2. ITTIL Research Memo by L. G. Wolfgang (to be published).

3. ITTIL Research Memo 309: "Noise in Multiplier Phototubes".

4. ITTIL Research Memo 397: "Star Tracking Limits of Performance".

5. N. P. Laverty "The Comparative Performance of Electron Tube Photodetectors in Terrestrial Space Navigation Systems", IEEE Tr. on Aerospace and Navigation Electronics, Vol. ANE-10, No. 3, September 1963, pages 194 - 205.

REFERENCES (Cont)

6. E. H. Eberhardt "Multiplier Phototubes for Single Electron Counting" paper presented at the Ninth Scintillation and Semiconductor Symposium, sponsored by the IEEE Prof. Group on Nuclear Science (to be published).

7. W. Atwill, Electronics, Sept. 30, 1960.

8. Allen "Astrophysical Quantities", 2nd Edition, 1963.

9. Project Balast, sponsored by the Air Force Cambridge Research Laboratories, under the direction of Prof. John Strong of Johns Hopkins University, Laboratory of Astrophysics.

10. R. K. H. Gebel, "Limitations for Daytime Detection of Stars Using the Intensifier Image Orthicon" Aerospace Research Laboratories Document ARL 64-46 Nov. 1963. (Conversion factor of 1.91 was computed from Curve XI, Fig 1, of this reference).

11. ITTIL Research Memo No. 398: "Smoothing Electron Multipliers".

APPENDIX I

LIST OF SYMBOLS AND APPROPRIATE UNITS*

B = sky brightness (lamberts)

D = effective diameter of optical system (cm)

f = "f"/number of optical system

F = focal length of optical system (cm)

h = dimension of one side of instantaneous sampling aperture (cm) (h x h area)

H = dimension of one side of image field at photocathode (cm) (H x H area)

I = illumination due to star at entrance aperture of optical system (phots)

L = image field illumination due to sky background brightness (phots)

n = number of photoelectrons per sampling time (sec^{-1})

Δn = increase in n due to star flux signal (sec^{-1})

t = sampling time per element (sec)

T = total search or frame time (sec)

W = star flux at photocathode image plane (lumens)

Q_{st} = effective quantum efficiency of photocathode for star flux (electrons/lumen second)

Q_{sk} = effective quantum efficiency of photocathode for sky brightness background flux (electrons/lumen second)

θ = viewed field angle (radians) (θ x θ total field)

e = electronic charge (coulombs)

I_{dc} = average dc current (amperes)

Δf = bandwidth (sec^{-})

i_n = noise current (amperes)

σ = average gain/stage of multiplier

k = multiplier noise factor

m = stellar magnitude

S/N = signal-to-noise power ratio

ϵ = absolute dissector counting efficiency ratio.

---

* (Based on a lumen, centimeter, coulomb, second system).